Research on the Smoke Diffusion with New Energy Vehicle Fire in Tunnel under the Action of Fine Water Mist and Longitudinal Ventilation

Zhenpeng Bai, Xiaohan Zhao, Jiali Zhang, Huaitao Song, Hengjie Qin, Haowei Yao

Abstract—**This paper explored the synergistic effect of fine water mist and longitudinal ventilation through a combination of numerical simulation and theoretical analysis. This paper established a new energy vehicle model driven by tunnels and lithium-ion batteries. It includes ventilation speed, fine water mist nozzle flow rate, fine water mist nozzle spacing, fire source location, and fire source heat release rate. This paper analyzed the temperature fluctuations, changes in carbon monoxide (CO) concentration, and smoke diffusion inside tunnels during simulated fire events. The results showed that as the wind speed gradually increases, the maximum temperature and total CO concentration below the ceiling of the tunnel gradually decrease. As the nozzle flow rate gradually increases, the cooling time becomes shorter and the cooling process becomes faster. The nozzle spacing gradually increases, and the maximum temperature below the ceiling of the tunnel decreases. As the HRR of the fire source gradually increases, the maximum temperature above the center of the tunnel rises, and the total concentration of CO gradually increases. This paper has important guiding significance for the smoke diffusion law of new energy vehicle fires in tunnels under the action of fine water mist and longitudinal ventilation.**

Index Terms—**Tunnel, Water mist, Longitudinal ventilation, Fire, New energy vehicle**

I. INTRODUCTION

The main cause of casualties in tunnel fires is suffocation [1]. The characteristics of smoke, especially its temperature, concentration, and propagation speed, have a significant impact on the evacuation process of personnel. The research background of smoke diffusion dynamics in tunnels during new energy vehicle fires is multifaceted when using fine water mist and longitudinal ventilation. It originates from the widespread use of tunnels, the uniqueness of tunnel fires, the surge of new energy vehicles and the increase in fire hazards caused by them, as well as the key role of longitudinal ventilation and fine water mist systems. This paper studies this phenomenon, which is of great significance for improving tunnel fire prevention and emergency response capabilities, ensuring personnel safety, optimizing tunnel design and operation management, and many other related aspects.

Matala et al. [1] conducted numerical simulations to investigate cable tunnel fires, focusing on fire propagation along power cables and the efficacy of water suppression in mitigating cable faults. Sliemon et al. [2] examined the impact of cable layer and spacing configurations on cable room fires, revealing a correlation between fire characteristics and cable placement. Gannouni et al. [3] utilized FDS fire simulation software to simulate tunnel fires under longitudinal ventilation, comparing calculated burnout lengths with simulated values using a predictive model. Their findings indicate that burnout layer arrival time is inversely related to heat release rate and directly related to longitudinal wind speed. Wang et al. [4] evaluated the effectiveness of water mist curtains (WMC) in preventing fire smoke spread. In subsequent work [5], they characterized smoke suppression efficiency using the water curtain momentum ratio, aiming to quantify smoke control and insulation effects in tunnel fires. Blanchard et al. [6] studied the interaction between fine water mist and hot air in longitudinally ventilated tunnels during fire events.

Zhang et al. [7] conducted experimental research on the impacts of longitudinal ventilation and fine water mist on heat transfer in tunnel fires using a scaled model tunnel. Their findings reveal that, while fine water mist can augment fire source combustion to a degree, it and the resulting water vapor effectively absorb and attenuate both radiative and total heat flux in tunnel spaces. Notably, this attenuation effect intensifies with increased fine water mist pressure. Cheong et al. [8] conducted a physical experiment to analyze the fire extinguishing characteristics of a low-pressure fine water mist system in the context of heavy vehicle fires in tunnels. Their results indicate that activating the system four minutes after ignition achieves excellent fire extinguishing effects, suggesting early activation for fire spread control. Additionally, they observed a positive correlation between

Manuscript received June 13, 2024. revised March 29, 2025. This work was supported by Key R&D and Promotion Special Project (Science and Technology Research) in Henan Province (252102241053), Doctor Scientific Research Fund of Zhengzhou University of Light Industry (2021BSJJ048), Henan Province Key R&D Special Project (231111322200).

Zhenpeng Bai is a lecturer in the Department of College of Building Environment Engineering, Zhengzhou University of Light Industry, China (E-mail: baiyi1056@126.com).

Xiaohan Zhao is a lecturer in the Department of Financial Management, Henan Light Industry Vocational College, China (Corresponding author to provide e-mail: xiaohanzhao1226@163.com).

Jiali Zhang is an undergraduate student at Department of College of Building Environment Engineering, Zhengzhou University of Light Industry, China (E-mail: zhangjiali0616@126.com).

Huaitao Song is an associate professor in the Department of College of Building Environment Engineering, Zhengzhou University of Light Industry, China (E-mail: songhuaitao@zzuli.edu.cn)

Hengjie Qin is an associate professor in the Department of College of Building Environment Engineering, Zhengzhou University of Light Industry, China (E-mail: walletjy@163.com)

Haowei Yao is an associate professor in the Department of College of Building Environment Engineering, Zhengzhou University of Light Industry, Zhengzhou, 450002, China (Co-Corresponding author to provide e-mail: yaohaowei@zzuli.edu.cn).

fine water mist flow rate and fire extinguishing efficacy. Zhong et al. [9] conducted comprehensive fire tests across three distinct fire heat release rates. Kalech et al. [10-11] employed numerical simulation methods to study smoke distribution and stratification in one-dimensional tunnel propagation under various ventilation conditions, identifying three flow layers: smoke, intermediate mixing, and fresh air. Notably, ventilation strategies exert differential effects on smoke flow temperature and velocity. Fine water mist technology utilizes high-pressure nozzles to disperse liquid fire extinguishing agents into minute droplets, interacting with flames to achieve fire extinguishment, suppression, or firefighting [12-13]. The author has conducted extensive research on fire and ventilation dynamics [14-19].

This article constructed models of highway tunnels and lithium-ion battery-powered new energy vehicles. Utilizing Pyrosim fire simulation software and Origin data visualization software, the study analyzed the temporal variation of temperature, longitudinal distribution of ceiling temperature, temporal variation of CO concentration, and smoke diffusion under various operational conditions. The results revealed distinct patterns of temperature change, CO concentration variation, and smoke behavior in tunnel fires under different scenarios.

II. Method

A. Physical Model

A typical new energy vehicle was selected as the research model, as shown in Fig. 1. The tunnel was 100 m long, 8 m wide, and 10 m high, with ventilation on both sides. The new energy vehicle was 4 m long, 2 m wide, and 2.6 m high.

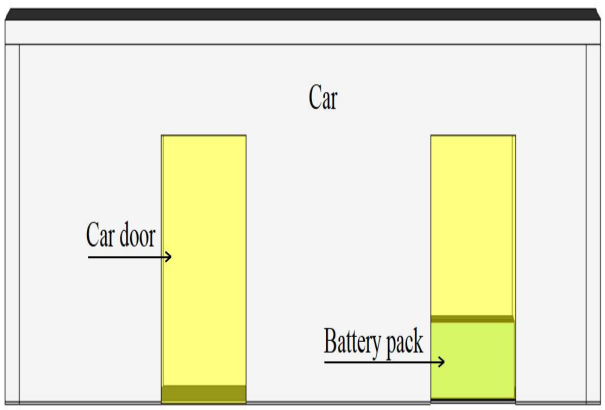

Fig. 1. A physical model new energy vehicle in the cable tunnel

B. Boundary conditions

To attain the primary research objectives, the model employed in this paper underwent simplification regarding the actual structural components of new energy vehicles. Notably, the vehicle roof structure was excluded to enhance the efficacy of fire suppression when utilizing fine water mist. Table 1 shows these simplifications, which encompass simulation conditions specifically designed to assess the fire extinguishment performance in cable tunnel environments.

TABLE 1 SIMULATION CONDITIONS OF CABLE TUNNEL WITH FIRE EXTINGUISH.

Case	Fire source Q (MW)	Nozzle spacing D (m)	Spray nozzle flow rate f (L/min)	Ventilation velocity v (m/s)
1	4	3	90	0
2	4	3	90	0.25
3	4	3	90	0.55
4	4	3	90	0.75
5	4	3	90	1
6	4	3	85	0.25
7	4	3	87	0.25
8	4	3	90	0.25
9	4	3	92	0.25
10	4	3	95	0.25
11	2.5	3	90	0.5
12	2.75	3	90	0.5
13	3	3	90	0.5
14	3.25	3	90	0.5
15	3.5	3	90	0.5
16	4	1.5	90	0.5
17	4	1.75	90	0.5
18	4	2	90	0.5
19	4	2.25	90	0.5
20	4	2.5	90	0.5

Ventilation openings were installed at the bilateral tunnel exits. Specifically, the ventilation opening positioned on the tunnel's right side remains functional, whereas the corresponding opening on the left side, despite being open, lacks power supply. Consequently, the right outlet functions as a gas supply outlet, and the left outlet operates as an exhaust outlet. This configuration establishes a longitudinal airflow direction from right to left within the tunnel. By modulating the wind speed emitted from the functional ventilation opening, the overall longitudinal wind speed inside the tunnel can be systematically regulated.

In the numerical simulation presented in this study, five distinct operational scenarios were designed. Within these scenarios, the fine water mist nozzle maintains a fixed position, whereas variables such as wind speed, flow rate of the fine water mist nozzle, heat release rate (HRR) of the fire source, and fire source location are altered. Specifically, the fine water mist nozzle is situated directly overhead the new energy vehicle, positioned 5 meters away from the tunnel walls, 9 meters beneath the tunnel ceiling, and 1 meter above the tunnel floor. Based on this configuration, two fine water mist nozzles are positioned on each lateral side of the vehicle, with a 3-meter spacing between them. Consequently, a total of five nozzles are arranged within the tunnel. These nozzles are designated as NOZZLE01, NOZZLE02, and NOZZLE04 from the center to the right, and NOZZLE01 (central), NOZZLE03, and NOZZLE05 from the center to the left.

A series of cases were investigated to examine the impact of varying the spacing between fine water mist nozzles. The sole parameter modified for the operational calculations was the distance separating the fine water mist nozzles, with no additional changes implemented. Throughout these cases, five fine water mist nozzles remained positioned 5 m away from the tunnel walls on both sides, 9 m beneath the tunnel ceiling, and directly on the tunnel floor.

III. Results And Discussions

A. The diffusion law of smoke from new energy vehicle fires in tunnels under different wind speeds

As shown in Fig. 2, the graph presents the temporal evolution of temperature for various wind velocities within a tunnel setting. Across all operational scenarios, the temperature profiles exhibited a linear increase, reaching a maximum temperature approximately 10 s prior to the activation of the fine water mist. Notably, Case 1 exhibited the highest temperature peak, approximately 180 ℃, whereas Case 5 demonstrated the lowest temperature peak, approximately 110 ℃.

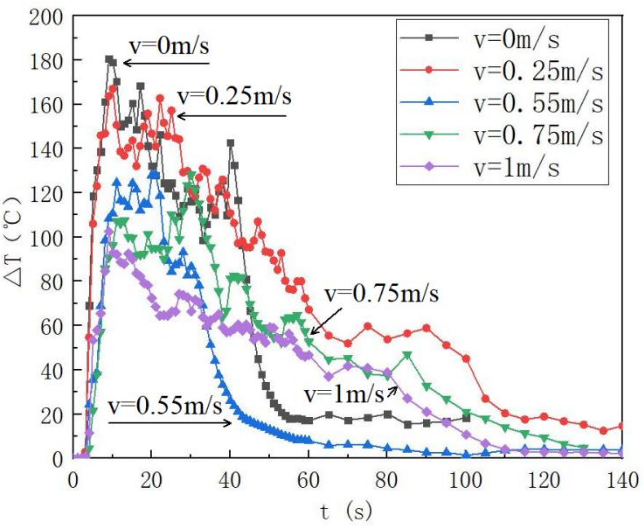

Fig. 2. Temperature variation over time under different wind speeds

After 10 s of fine water mist activation, the tunnel ceiling temperature undergoes a rapid decrease under varying wind speed conditions. The temperature measurements obtained from thermocouples can be categorized into two distinct stages: a rapid cooling phase and a slow cooling phase. Upon release, the fine water mist droplets swiftly interact with hot air, absorbing substantial heat through evaporation, thereby initiating the rapid cooling phase. Subsequently, the mist droplets disperse and propagate throughout the space. As time progresses, the distance between droplets increases, reducing their interfacial contact with the surroundings. This dispersion and movement diminish the efficacy of evaporative cooling, giving rise to the slow cooling phase. In Fig. 2, the period from 10 to 60 s corresponds to the rapid cooling phase, whereas 60 to 140 s represents the slow cooling phase. Consequently, based on the analysis, it is concluded that the peak temperature recorded by the thermocouples decreases with increasing wind speed. This observation is attributed to the accelerated airflow within the tunnel, which facilitates the prompt removal of heat generated by the fire, thus achieving a more rapid temperature reduction.

As shown in Fig. 3, it is the effect of the longitudinal temperature distribution below the tunnel ceiling at 60 seconds. As the wind speed gradually increases, the highest temperature measured by the thermocouple above the center of the tunnel decreases, and the downward trend of temperature from the middle to the end becomes more stable.

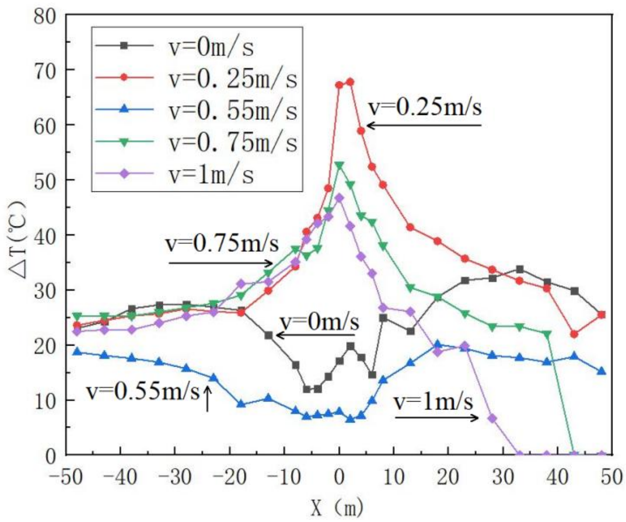

Fig. 3. Longitudinal distribution of tunnel ceiling temperature at 60 seconds under different wind speeds

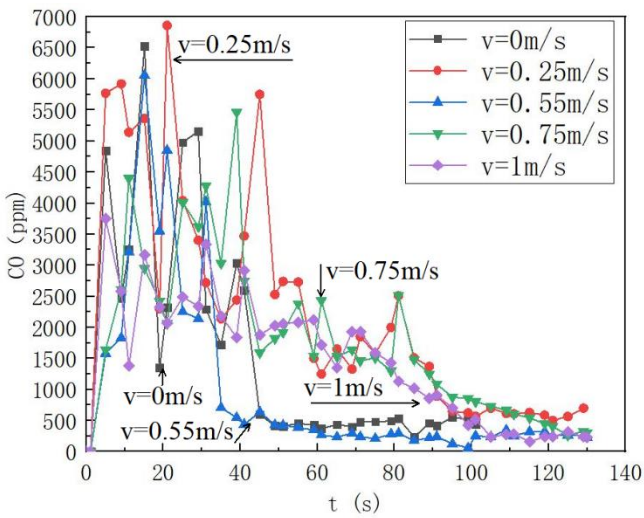

Fig. 4. Changes in CO over time under different wind speeds

As shown in Fig. 4, the variation of CO concentration in the ceiling over time under different wind speed conditions is displayed. Before applying fine water mist, the concentration of CO increased linearly under all operating conditions. In the early stages of fine water mist application, each curve showed significant fluctuations. The fluctuation levels of operating situations 1 and 2 are relatively large, while the fluctuation level of situation 5 is relatively small. As the wind speed gradually increases, the fluctuation of CO concentration gradually decreases, and the overall concentration of CO gradually decreases.

In cases 1 and 2, the smoke dispersion on the tunnel's right side is notably greater compared to the relatively limited dispersion observed on the left side. Conversely, in case 5, the smoke dispersion extent on the tunnel's right side diminishes, whereas the amplitude of smoke dispersion on the left side becomes relatively pronounced. The rate of smoke diffusion exhibits an increase from case 1 to case 5. Consequently, as the wind velocity gradually augments, the smoke dispersion range on the tunnel's right side decreases, the smoke dispersion amplitude on the left side escalates, and the overall rate of smoke diffusion intensifies.

B. The diffusion law of smoke from new energy vehicle fires in tunnels under different water mist systems

As shown in Fig. 5, it presents the temporal variation of temperature under various nozzle flow rates of fine water mist. Prior to the activation of the fine water mist, the temperature distributions across all conditions remain essentially uniform, exhibiting a linear upward trend. Within the first 10 s following activation, no substantial temperature reduction is observed. However, approximately 25 s later, a notable decline in temperature initiates across all five scenarios, with case 10 exhibiting the most significant temperature drop. After approximately 40 s, the temperature reduction attains approximately 20 ℃. Through analytical examination, it is concluded that the flow rate of the fine water mist nozzle has a considerable influence on the cooling effect on the ceiling temperature at the fire source. Specifically, a higher nozzle flow rate results in a shorter cooling duration and a more rapid cooling process.

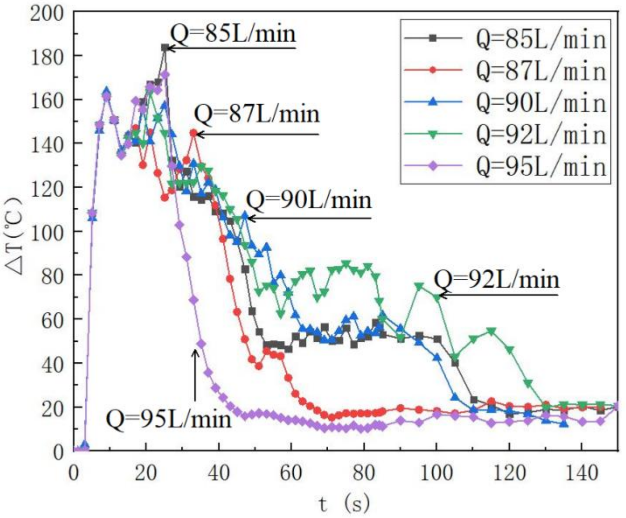

Fig. 5. Temperature variation over time under different nozzle flow rates under different water mist systems

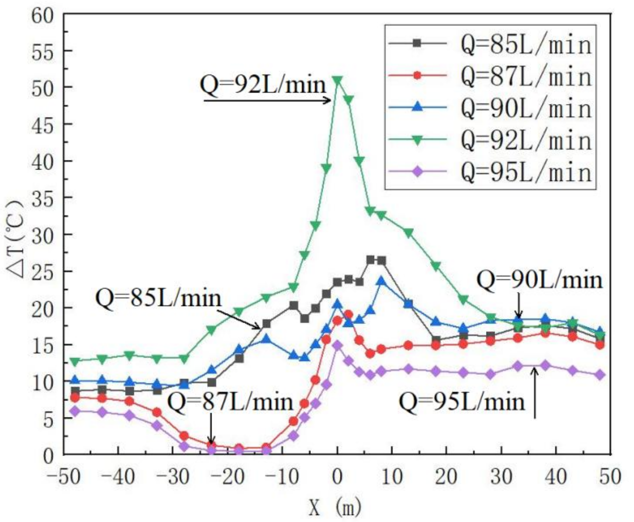

Fig. 6. Longitudinal distribution of tunnel ceiling temperature at 110 seconds under different water mist systems

As shown in Fig. 6, the graphic depicts the longitudinal distribution of tunnel ceiling temperature at 110 s for various fine water mist systems. At this time point, case 9 exhibits the highest maximum temperature, accompanied by the most pronounced downward trend from the tunnel's center to its end. Conversely, case 5 displays the lowest maximum temperature, with the most stable downward trend from the center to the end. Analytical insights indicate that during the initial stage of fine water mist application, as the nozzle flow rate increases, the peak temperature recorded by the thermocouple positioned above the tunnel's center rises, and the temperature decline from the middle to the end becomes more evident. However, in the subsequent stage of fine water mist application, the maximum temperature of the ceiling thermocouple may not escalate with an increase in nozzle flow rate; nonetheless, the overall temperature trend from the center to the end continues to exhibit a downward pattern.

As shown in Fig. 7, the figure illustrates the temporal variation of CO concentration at the ceiling under various nozzle flow rates. Specifically, at a nozzle flow rate of 85 L/min, the CO concentration had escalated to approximately 6000 ppm prior to the application of fine water mist. Subsequent to the application, the CO concentration exhibited a gradual decline and ultimately stabilized at around 1700 ppm.

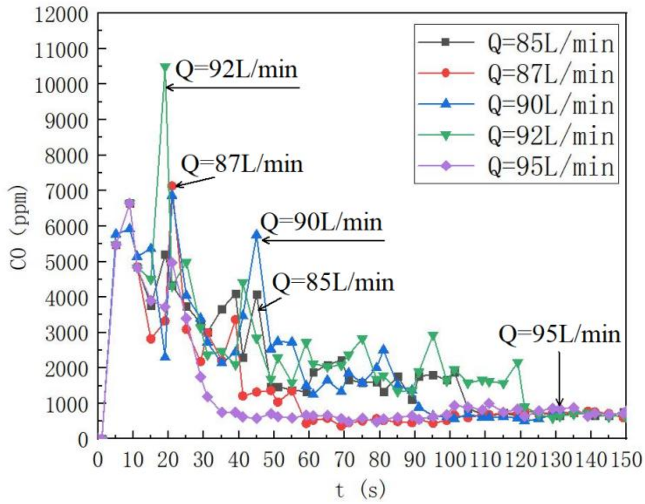

Fig. 7. CO variation over time under different nozzle flow rates under different water mist systems

This paper explores the smoke diffusion law under different nozzle flow rates. At 60 s, the temperature drop trend of cases 6-10 gradually stabilizes. This article studies the smoke diffusion law at 60 s. The smoke height layer in case 6 is higher, while the smoke thickness layer in case 10 is lower. From case 6 to case 10, the height layer of smoke gradually decreases. Therefore, it can be concluded from the analysis that the height layer of smoke gradually decreases with the increase of the flow rate of the fine water mist nozzle. Due to the potential increase in momentum of water mist, it helps to compress the smoke layer downwards, bringing it closer to the ground.

As shown in Fig.8, the variation of CO concentration in the ceiling over time was observed at different nozzle spacings. Before the fine water mist is activated, the CO concentration increases linearly under all operating conditions. In the initial stage of fine water mist application, each curve shows significant fluctuations. At a nozzle spacing of 2.5 m, the CO concentration rises to approximately 3500 ppm before applying fine water mist. In the initial stage of applying fine water mist, the CO concentration still maintains an upward trend and reaches a peak of about 5700 ppm within about 20 s. Subsequently, the concentration of CO began to decrease. As the fine water mist continues to act, the CO concentration decreases to about 100 ppm.

As the spacing between the fine water mist nozzles increases progressively, the height of the smoke layer undergoes a gradual elevation. This phenomenon can be attributed to the insufficient momentum of the water mist to exert a significant impact on the smoke, resulting in greater instability within the smoke layer and consequently, an increase in its height.

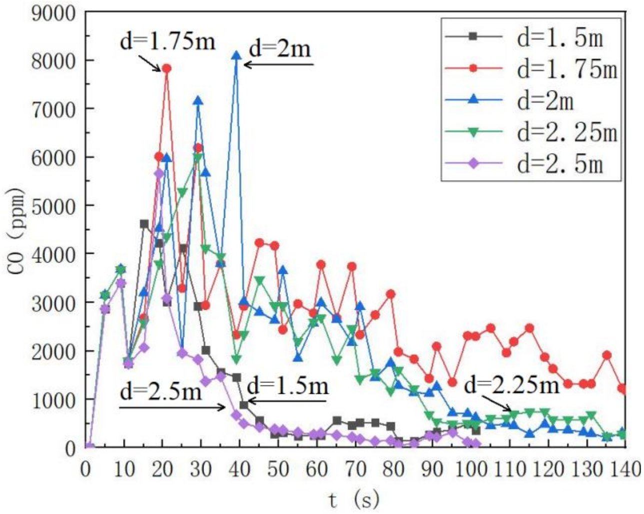

Fig. 8. CO variation over time under different nozzle spacing under different nozzle flow rates

C. The diffusion law of smoke from new energy vehicle fires in tunnels under different fire sources

As shown in Fig. 9, the figure depicts the temporal variation of temperature under different heat release rates (HRRs) of the ignition source. An analysis was conducted on the temperature distribution recorded by ceiling thermocouples under varying HRR conditions of the fire sources. Prior to the activation of fine water mist, all cases exhibited a similar linear increase in temperature curves. The peak temperature was observed approximately 10 s after the commencement of the experiment, with case 15 reaching the highest temperature of approximately 125 ℃ and case 11 achieving the lowest temperature of around 90 ℃. The maximum temperatures observed in cases 12, 13, and 14 are directly correlated with the increase in the HRR of the fire source. Following the activation of fine water mist after 10 seconds, a notable decrease in temperature was observed across all five cases, with case 11 exhibiting the most significant drop. At approximately 40 s, the temperature of case 11 decreased to around 25 ℃, whereas the temperature of case 15 declined at the slowest rate. From case 11 to case 15, the rate of temperature decrease gradually diminishes. A comprehensive analysis of the data concludes that a higher HRR of the fire source results in a higher maximum temperature, a longer cooling time required, and a slower cooling process.

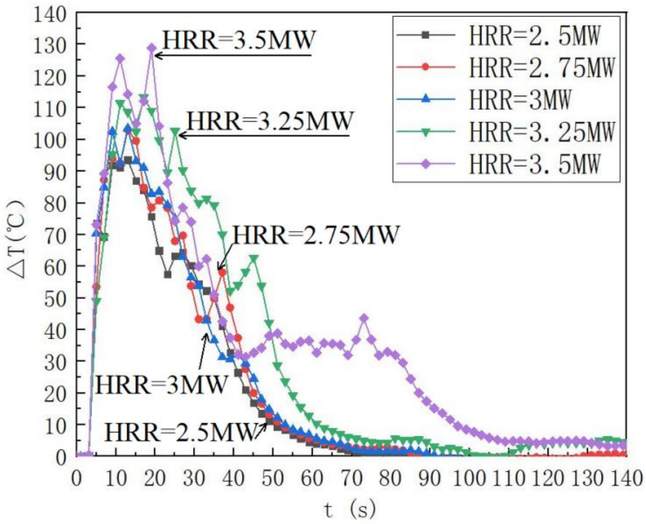

Fig. 9. Temperature variation over time under different fire source HRRs

After the application of fine water mist, the temperature distribution within the tunnel exhibits a distinctive pattern, characterized by lower temperatures at both ends and a higher temperature in the middle section. Specifically, the thermocouple positioned above the new energy vehicle registered the highest temperature, whereas the thermocouple situated at the tunnel's terminus recorded the lowest temperature. As an individual traverses from the tunnel's center towards either the left or right end, a distinct downward trend in temperature is evident. Furthermore, it was observed that the peak temperature achieved is positively correlated with the power of the fire source; in other words, an increase in the fire source's power results in an elevation of the maximum temperature. Additionally, as one moves from the center to the end of the tunnel, an augmentation in the fire source's power leads to a more pronounced decrease in temperature.

As shown in Fig. 10, the longitudinal distribution of tunnel roof temperature at the 50 s is depicted. At this point in time, the highest temperature observed in case 15 showed the most significant trend, while case 11 had the lowest temperature and the most stable trend. Based on this analysis, it can be concluded that there is a direct correlation between the HRR of the fire source and the maximum temperature reached. Specifically, as the HRR of the fire source increases, the maximum temperature will also rise. In addition, when people move from the middle to the end of the tunnel, a significant decrease in temperature is observed, which is more pronounced at higher HRR values.

As shown in Fig. 11, the variation of CO concentration in the tunnel roof over time under different heat release rates is displayed. Before applying fine water mist, a linear increase in CO concentration was observed in all cases. In the initial application of fine water mist, each curve exhibits significant fluctuations, with case 15 showing the maximum degree of fluctuation and case 11 showing the minimum degree of fluctuation. When the HRR is 3 MW, the CO concentration rises to about 3700 ppm before introducing fine water mist. In the early stages of fine water mist application, the concentration of CO continues to increase, reaching a peak of approximately 6000 ppm within about 20 s. With the continuous application of fine water mist, the concentration of CO gradually decreases and eventually stabilizes at about 0ppm. These findings indicate that although the initial use of fine water mist may cause temporary fluctuations in CO concentration, continued use of fine water mist can effectively reduce and stabilize CO levels in tunnel ceilings.

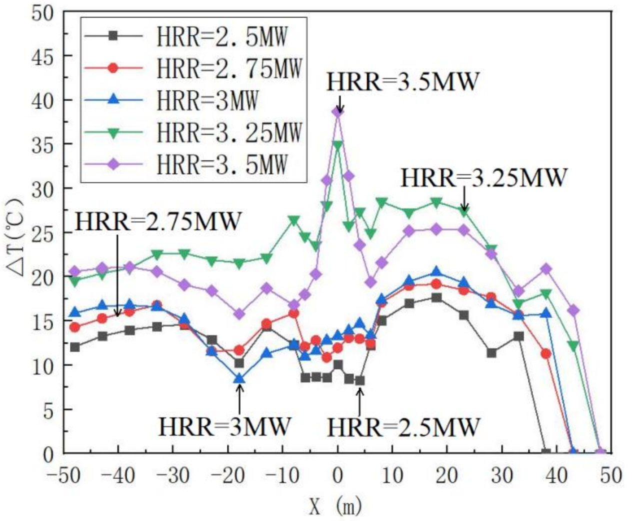

Fig. 10. Longitudinal distribution of tunnel ceiling temperature at 50 seconds

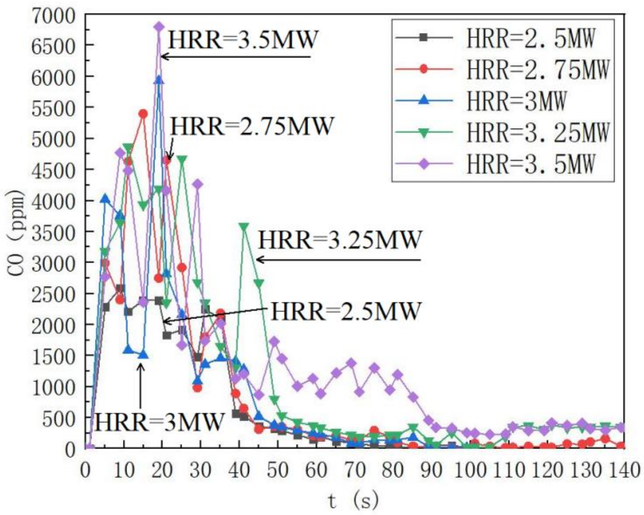

Fig. 11. Changes in CO over time under different fire source HRRs

In case 11, the smoke dispersion is relatively limited, and the quantity of smoke produced is correspondingly small. Conversely, in case 15, the smoke dispersion range is relatively extensive, and the quantity of smoke generated is notably higher. From case 11 to case 15, there is an increase in the quantity of smoke produced, accompanied by an expansion in the dispersion range and a gradual acceleration in the diffusion rate. Through analysis, it can be concluded that as the HRR of the fire source progressively increases, the quantity of smoke generated also augments, and both the diffusion speed and range exhibit an increase.

IV. Conclusions

This paper employs numerical simulation techniques to investigate the variations in fire parameters associated with new energy vehicles within tunnel environments, particularly when influenced by fine water mist and longitudinal ventilation. A comprehensive simulation model was developed utilizing Pyrosim software, encompassing tunnels, new energy vehicles, ventilation systems, fine water mist fire suppression systems, and data acquisition systems. The grid size was meticulously determined and validated to guarantee its appropriateness for the simulation tasks. Five distinct fire experiments were simulated under varying operational conditions, enabling the examination of the temporal evolution of roof temperature, vertical distribution of roof temperature, temporal distribution of CO concentration, and patterns of smoke dispersion. These investigations centered on five crucial parameters: wind speed, fine water mist nozzle flow rate, fine water mist nozzle spacing, heat release rate (HRR) of the fire source, and fire source location. The main conclusions of this article are as follows:

(1) At varying wind speeds, the maximum temperature recorded by the thermocouple positioned above the tunnel's center exhibits a declining trend as wind speed incrementally increases. The temperature decrease from the tunnel's midpoint to its terminus becomes more consistent. Concurrently, the overall concentration of CO diminishes gradually. The smoke diffusion range diminishes on the tunnel's right side while augmenting on its left side, leading to an overall acceleration in the diffusion rate.

(2) When considering different nozzle flow rates, an increase in the flow rate results in a shortened cooling time and an accelerated cooling process. The decline in temperature from the tunnel's center to its end becomes more pronounced. During the later stages of fine water mist application, the maximum temperature recorded by the ceiling thermocouple may cease to escalate with further increases in nozzle flow rate; however, a downward temperature trend persists from the midpoint to the tunnel's end. The impact of nozzle flow rate on CO concentration is insignificant, with each curve demonstrating comparable fluctuation levels. Additionally, the smoke layer's height diminishes progressively.

(3) At differing nozzle spacings, an increase in spacing leads to a decrease in the maximum temperature measured by the thermocouple. The temperature decline from the tunnel's center to its end becomes more stable. Concurrently, the overall concentration of CO gradually increases, and the smoke layer's height rises progressively.

(4) Under varying HRR conditions, an increase in the HRR of the fire source results in a higher maximum temperature recorded by the thermocouple above the tunnel's center, a prolonged cooling time, and a slower cooling process. The temperature decrease becomes more pronounced from the tunnel's midpoint to both ends. The overall concentration of CO gradually increases. Furthermore, the quantity of smoke generated escalates, accompanied by an increase in both diffusion speed and range.

References

[1] A. Matala, and S. Hostikka. “Probabilistic simulation of cable performance and water based protection in cable tunnel fires”. *Nuclear Engineering and Design*, vol. 241, no. 12, pp. 5263-5274, 2011.

[2] M. Siemon, O. Riese, B. Forell, D. Krönung, and W. Klein-Heßling. “Experimental and numerical analysis of the influence of cable tray

arrangements on the resulting mass loss rate and fire spreading". *Fire and Materials*, vol. 43, no. 5, pp. 497-513, 2019.

[3] S. Gannouni, and R. Maad. "Numerical analysis of smoke dispersion against the wind in a tunnel fire". *Journal of Wind Engineering & Industrial Aerodynamics*, vol. 158, pp. 61-68, 2016.

[4] Z. Wang, X. Wang, Y. Huang, C. Tao, and H. Zhang. "Experimental study on fire smoke control using water mist curtain in channel". *Journal of hazardous materials*, vol. 342, pp. 231-241, 2018.

[5] Z. Wang, X. Jiang, Q. Wang, and B. Wang. "Numerical investigation of water curtain for smoke blocking and heat insulation in urban underground road". *Thermal Science and Engineering Progress*, vol. 35, pp. 101468, 2022.

[6] E. Blanchard, P. Boulet, P. Fromy, S. Desanghere, P. Carlotti, J. Vantelon, and J. Garo. "Experimental and numerical study of the interaction between water mist and fire in an intermediate test tunnel". Fire Technology, vol. 50, pp. 565-587, 2014.

[7] Y. Zhang, K. Zhang, L. Chen, et al. "Experimental study on heat transfer of tunnel fire under the influence of longitudinal ventilation and water mist system". *Fire And Materials*, vol. 45, no. 6, pp. 772-778, 2021.

[8] M. Cheong, W. Cheong, K. Leong, et a1. "Heat release rate of heavy goods vehicle fire in tunnels with fixed water based fire-fighting system". *Fire technology*, vol. 50, no. 2, pp. 249-266, 2014.

[9] M. Zhong, C. Shi, L. He, J. Shi, C. Liu and X. Tian. "Smoke development in full-scale sloped long and large curved tunnel fires under natural ventilation". *Applied Thermal Engineering*, vol. 108, pp. 857-865, 2016.

[10] B. Kalech, Z. Mehrez, M. Bouterra, et al. "Temperature stratification in a road tunnel". *Thermal Science*, vol. 20, no. 1, pp. 223-237, 2016.

[11] B. Kalech, M. Bouterra, and A. ElCafsi. "Numerical analysis of smoke flow under the effect of longitudinal airflow in a tunnel fire". *Fire and Materials*, vol. 44, no. 8, pp. 1033-1043, 2020.

[12] R. Carvel, A. Beard, P. Jowitt, and D. Drysdale. "Variation of heat release rate with forced longitudinal ventilation for vehicle fires in tunnels". *Fire Safety Journal*, vol. 36, no. 6, pp. 569-596, 2001.

[13] J. Mawhinney, B. Dlugogorski, and A. Kim. "A closer look at the fire extinguishing properties of water mist". *Fire Safety Science*, vol. 4, no. 1, pp. 47-60, 1994.

[14] Z. Bai, H. Yao, and H. Zhang. "Experimental study on fire characteristics of cable compartment in utility tunnel with fire source at shaft side". *Engineering Letters*, vol. 30, no. 2, pp. 806-810, 2022.

[15] Z. Bai, Y. Yu, K. Lv, H. Qin, H. Yao and C. Yang. "Experimental study on influence of natural ventilation on near wall fire in cable Tunnel". *Engineering Letters*, vol. 31, no. 2, pp. 689-694, 2023.

[16] Z. Bai, Y. Yu, J. Zhang, H. Hu, M. Xing, and H. Yao. "Study on fire characteristics of lithium battery of new energy vehicles in a tunnel". *Process Safety and Environmental Protection*, vol. 186, pp. 728-737, 2024.

[17] Z. Bai, H. Yao, and H. Zhang. "Experimental study on fire characteristics in cable compartment of utility tunnel with natural ventilation". *Plos One*, vol. 17, no. 4, pp. e0266773, 2022.

[18] Z. Bai. "Burning characteristics of power cables with cone calorimeter." *Heliyon*, vol. 10, no. 3, pp. e25103, 2024.

[19] Z. Bai, Y. Yu, Y. Liu, H. Qin, H. Yao. "Optimization analysis of influencing factors of water mist system in utility tunnel based on orthogonal tests". *Applied Thermal Engineering*, vol. 267, pp. 125814, 2025.